

Mini review

Recent Advancement in the development of hybridization chain reaction-based electrochemiluminescence biosensors

Ting Sun¹, Jia Du², Zhuo Li¹, and Feng Zhao^{1,*}

¹ School of Chemistry and Materials Sciences, Guizhou Integrated Research Center of Polymer Electromagnetic Materials, Key Laboratory of Functional Organic Molecule, Guizhou Education University, Guiyang 550018, China

² Technology Center for China Tobacco Henan Industrial Limited Company, Zhengzhou, Henan, 450000, China

*E-mail: fygu2010@163.com

Received: 15 February 2022 / Accepted: 6 April 2022 / Published: 7 May 2022

Electrochemiluminescence (ECL) biosensors have been widely used in bioassays due to their high sensitivity, fast response, simple equipment and low cost. Signal amplification is an important means to improve the sensitivity of ECL biosensors. The common enhancement strategies include DNA amplification, enzyme-assisted signal enhancement, nanomaterials-based amplification, and the application of redox-active probes and luminophores. Among them, hybridization chain reaction (HCR) shows simple experiment operation and high amplification efficiency, which can be integrated with various detection technologies for signal enhancement. This paper mainly summarizes the application of HCR amplification in the design of ECL biosensors.

Keywords: Hybridization chain reaction; electrochemiluminescence biosensor; signal amplification; nanomaterials

1. INTRODUCTION

Electrochemiluminescence (ECL) is a combination of electrochemistry and chemiluminescence, including electrochemical excitation and light radiation. The electrochemical reaction provides active intermediates and excited light sources. In the subsequent luminescence relaxation process, the excited luminophore returns to the ground state and produce an ECL signal. Since there is no need to excite the light source, ECL can break through the limitation of background interference in photoluminescence system. Thus, it has the advantages of electrochemical controllability and high sensitivity of chemiluminescence analysis. In ECL electrochemical reaction, the time and position of luminescence

reaction can be controlled by the used potential. The generation of the excited state in ECL can be selectively controlled by changing the potential. In most cases, the ECL emitters can be regenerated after excitation, making ECL biosensor be a lossless technology. ECL biosensors have been widely used in biological analysis because of their high sensitivity, fast response, simple equipment and low cost [1-3]. Signal amplification is an important means to improve the sensitivity of bioassays. The commonly used strategies for improving the sensitivity include DNA amplification, enzyme-assisted signal enhancement, nanomaterials-based amplification, and the application of redox-active probes and luminophores [4]. DNA amplification technology mainly includes two categories: one is enzyme-mediated signal amplification (e.g. polymerase chain reaction, rolling ring isothermal amplification and strand displacement amplification) [5], and the other is enzyme-free isothermal amplification such as hybridization chain reaction (HCR) proposed by Dirks and Pierce in 2004 [6]. Among them, HCR shows simple experiment operation and high amplification efficiency, which can be performed at room temperature without the use of enzyme [7, 8]. The HCR has high compatibility with various detection technologies such as fluorescence, electrochemistry, chemiluminescence and colorimetry [9]. This paper mainly summarizes the applications of HCR-based amplification technology in the ECL detection of different analytes, including nucleic acids, proteins, enzymes, small molecules, tumor cells, and so on. Usually, the signal output and enhancement is combined with other amplification strategies, such as natural enzymes, artificial enzymes, small luminophores and nanomaterials.

2. HCR-BASED ECL METHODS

2.1 Enzymatic amplification

Natural enzymes possess high catalytic activity and excellent substrate selectivity, which have been extensively utilized in bioassays for target recognition and signal transformation. Through labeling of the hairpins with enzymes, the HCR products (long dsDNA chains) can capture many enzymes to generate a large number of redox-active species, thus enhancing the ECL signal. For example, glucose oxidase (GOx) can catalyze the oxidation of glucose in the presence of dissolved O₂ to in-situ generate H₂O₂ [10, 11]; Xiao et al. reported an ECL biosensor for immunoassays of IgG through the HCR and GOx-based signal amplification [12]. After the sandwich-type immunoreaction, tetrameric streptavidin (SA) proteins were introduced to connect biotin-labeled initiator and biotinylated anti-IgG via the SA-biotin interactions. In the presence of GOx-conjugated ssDNA and complementary strand, HCR occurred and numerous GOx molecules were immobilized on the surface of the electrode. A large amount of H₂O₂ molecules were in-situ generated, thus enhancing the ECL intensity of luminol. Meanwhile, they employed the cascade catalysis of GOx and HRP to in-situ generate dissolved O₂ as the co-reactant of S₂O₈²⁻ [13]. Nonetheless, the use of fragile enzymes as the signal reporters suffers from several problems such as poor stability, complicated preparation step, easy inactivation and high cost.

2.2 DNAzymes-based amplification

DNAzymes are functional oligonucleotides with enzymatic properties, which have been widely used to develop biosensors. Compared with natural enzymes, DNAzymes are more stable, less expensive and easier to be modified. Hemin/G-quadruplex DNAzyme produced by the insertion of hemin into a G-rich oligonucleotide shows the HRP-like catalytic ability. By coupling G-rich oligonucleotide with hairpin DNA, dsDNA polymers formed by HCR can capture a large amount of hemin/G-quadruplexes into the DNAzyme nanowires. They catalyzed the decomposition of H_2O_2 to quickly generate abundant reactive oxygen species (ROSs), which could significantly enhance the ECL intensity. Liu et al. developed a biosensor for silver ions detection based on hemin/G-quadruplex DNAzyme nanowires-catalyzed luminol ECL system [14]. The presence of silver ions resulted in the release of nanowires from the electrode surface through the formation of a stable $\text{C-Ag}^+\text{-C}$ complex, causing a decreased ECL intensity. Besides, hemin/G-quadruplex can also catalyze the reduction and depletion of dissolved O_2 and quench the ECL emission of the $\text{O}_2/\text{S}_2\text{O}_8^{2-}$ system. Based on this property, Jiang et al. reported a signal-on ECL biosensor for the detection of methyltransferase activity [15].

Hemin in DNAzyme exhibits excellent redox reversibility due to the reversible redox of $\text{Fe}^{\text{III}}/\text{Fe}^{\text{II}}$. Zhang et al. demonstrated that hemin could act as electrochemically regenerable co-reaction accelerator to catalyze the peroxydisulfate ($\text{S}_2\text{O}_8^{2-}$)-based system and amplify the ECL signal [16]. Zeng et al. reported a 3,4,9,10-perylenetetracarboxylic acid (PTCA)-based ECL biosensor for Aflatoxin M1 detection using hemin/G-quadruplex nanowire as co-reaction accelerator [17]. In this work, the glassy carbon electrode (GCE) was modified with PTCA and AuNPs. Through target-catalyzed hairpin assembly (CHA) and HCR, Aflatoxin M1 could stimulate the generation of dendritic DNA polymers. After the introduction of hemin, plenty of hemin/G-quadruplex structures were produced on the dendritic DNA polymers and significantly improved the ECL intensity in the PTCA/ $\text{S}_2\text{O}_8^{2-}$ system.

2.3 DNAzymes-based amplification

It is a common and facile strategy to label the DNA probe with a functional molecule for signal output. By using ECL luminophore-conjugated DNA hairpins, dsDNA polymers generated from HCR have many luminophores, thus leading to the increase of ECL signal [18, 19]. To reduce the positive or negative errors, Zhu et al. developed a ratiometric biosensor for the detection of miRNA-133a through a DNA tetrahedron nanostructure (DTN) and HCR dual amplification strategy [20]. In this work, thiol-modified DNA tetrahedron nanostructure was utilized to immobilize HCR trigger on the gold electrode. Two $\text{Ru}(\text{bpy})_3^{2+}$ -labeled hairpins (H1 and H2) were employed as fuel strands for HCR. A hairpin DNA tagged with methylene blue (MB) was hybridized with the capture sequence of DTN. In the presence of target miRNA-133a, the coupling of target and MB-labeled hairpin initiated HCR and many luminophores were bound to the electrode, generating an amplified ECL signal. Meanwhile, MB molecules produced stable electrochemical signal as an internal reference signal. Besides, Zhang et al. reported an ECL biosensor for miRNA detection by labeling of hairpins with ferrocene (Fc) to decrease the ECL emission of luminol-functionalized Au NPs@ZnO through competitive depletion of dissolved O_2 [21]. Recently, Wang et al. developed a HCR-based ratiometric biosensor for the determination of

miRNA-133a by using zinc-metal organic frameworks (Zn-MOFs) as the coreactant-free ECL luminophores [22]. As shown in Figure 1, the Zn-MOFs were synthesized with 4'-(4-carboxyphenyl)-2,2':6'',2''-terpyridine (Hcptpy) as the organic luminescence ligand and zinc as the metal node. Compared with Hcptpy, the Zn-MOFs displayed excellent annihilation and coreactant ECL emission. Two DNA hairpins were labeled with N,N-diethylethylenediamine (DEAEA). After HCR, lots of DEAEA were immobilized on the electrode, resulting in the enhanced anodic ECL intensity of Zn-MOFs. Dopamine (DA) can be used to modify DNA as an excellent ECL quencher. Li et al. reported the ECL detection of miRNA-141 based on branched HCR (bHCR). As shown in Figure 2, a terbium(II) organic gel (TOG) was prepared and used as the ECL luminophore to modify the electrode and immobilize SA-labeled AuNPs. After bHCR, the formed two-layered bHCR circuit was captured by SA on the electrode. DA molecules were oxidized by the strong oxidant $\text{SO}_4^{\cdot-}$. The oxidation product, o-benzoquinone species, could accept the energy from the excited state of TOG to cause the decrease of ECL signal.

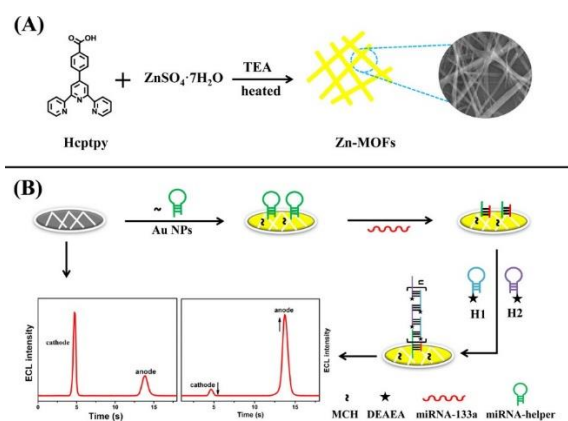


Figure 1. Schematic representation of (A) synthesis of Zn-MOFs and (B) illustration of the coreactant-free ratiometric ECL biosensor for detecting miRNA-133a [22]. Copyright 2021 American Chemical Society.

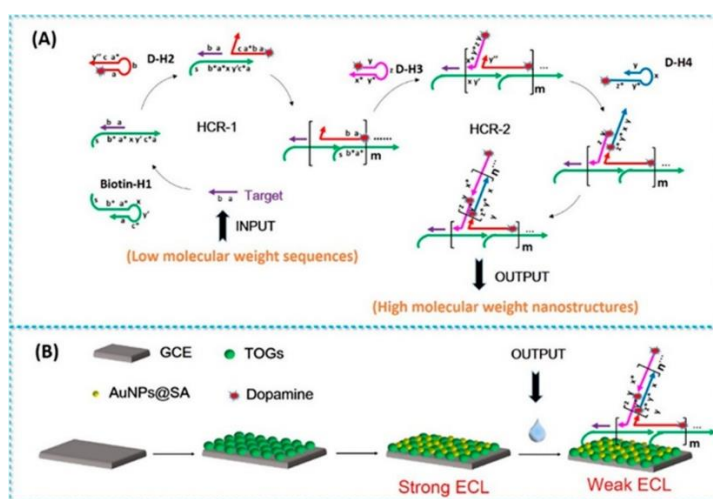


Figure 2. Schematic representation of (A) dual signal amplification bHCR strategy triggered by miRNA-141 and (B) Fabrication process of the biosensor based on the one-step introduction approach [23]. Copyright 2019 American Chemical Society.

Because of the high ECL efficiency, several ECL luminophores have been widely applied to develop label-free HCR-based ECL biosensors by insertion into the dsDNA groove [24-27]. For example, Zhang et al. developed a signal-on ECL aptasensor for bisphenol A based on HCR and electrically heated electrode [28]. In this work, the presence of bisphenol A led to the departure of aptamer and the residual capture DNA could induce HCR to generate long dsDNA on the electrode. The resulting dsDNA was then intercalated with many $\text{Ru}(\text{phen})_3^{2+}$ as the ECL emitter to produce an enhanced ECL signal. Meanwhile, the temperature controlled by electrically heated electrode not only regulated the process of target recognition and HCR, but also increased the performance of the ECL aptasensor.

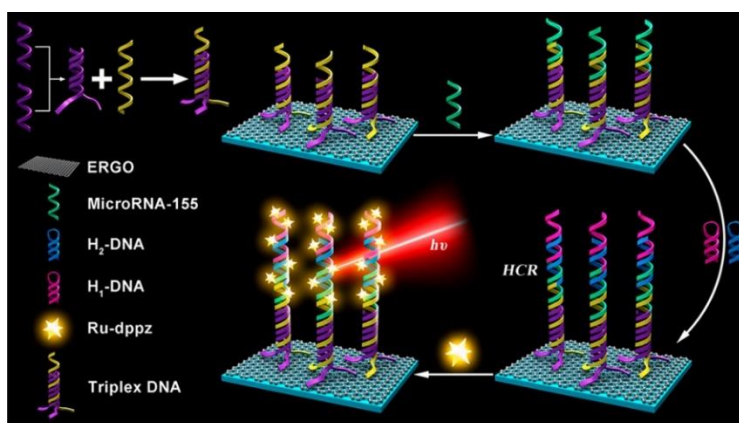


Figure 3. Schematic representation of the stepwise fabrication of the ECL biosensor with a tripod probe [29]. Copyright 2019 American Chemical Society.

Most of the above biosensors involve the direct formation of long dsDNA through HCR on the electrode surface. This may suffer from the shortcomings including time consuming and low assembly efficiency due to probe tangle and steric hindrance. To overcome these disadvantages, Lu et al. developed an ECL biosensor with a tripod probe for miRNA-155 detection [29]. As displayed in Figure 3, three ssDNA strands with A-rich sequence (AAAAAAA-) were hybridized with triple-stranded-DNA (tsDNA) and then assembled on the electrodeposited reduced graphene oxide-modified GCE (ERGO/GCE) through π - π stacking interactions. The employment of the tsDNA-based platform could enhance the accessibility of the probe and ensure effective capture of the target. In the presence of miRNA-155, many extended dsDNA chains were formed and the ECL luminophore $[\text{Ru}(\text{bpy})_2(\text{dppz})]^{2+}$ (bpy, 2,2'-bipyridine; dppz, dipyrido[3,2-a:2',3'-c]phenazine) could be intercalated into the dsDNA, producing an amplified ECL signal in the presence of the co-reactant.

HCR in homogeneous solution is convenient and efficient, which can shorten the reaction time and improve the amplification effect [30, 31]. Huang et al. reported an ECL biosensor for pyrophosphatase (PPase) detection based on click chemistry-triggered HCR in homogeneous solution [32]. As shown in Figure 4, pyrophosphate (PPi) could be coordinated with Cu^{2+} ions to form a complex ($\text{PPi}/\text{Cu}^{2+}$). In the presence of PPase, PPi was hydrolyzed into orthophosphate (Pi) to release Cu^{2+} ions from the complex. Then, the free Cu^{2+} ions were reduced to Cu^+ ions by sodium ascorbate which could catalyze the ligation of two ssDNA strands modified with alkyne and azide groups at the end. The long

nanomaterials with different components and morphologies have been extensively applied in the development of PEC biosensors, including metal nanoparticles, carbon-based nanomaterials, quantum dots (QDs), and metal organic frameworks (MOFs). Nanomaterials used as the labels for signal amplification can be briefly classified into three categories: nanoemitters, nanocarriers to load signal reporters, and nanocatalysts to accelerate the ECL reaction.

Besides conventional ECL reagents such as luminol and metal complexes, many nanomaterials have been utilized as novel luminophores to construct different ECL biosensors. For example, QDs have received intensive attention because of their tunable optical properties and stable ECL signals [34, 35]. Ge et al. developed a biosensing platform for “on-off” detection of thrombin and miRNA [36]. In this work, after the bipedal molecular machine-triggered surface programmatic chain reaction, numerous QDs were tethered alongside with dsDNA polymers, and silver ions captured by C-rich DNA acted as the coreation accelerators to obviously increase the ECL signal for thrombin detection. However, when numerous silver ions were released from mesoporous silica nanoparticles triggered by miRNAs, the in-situ formed silver nanoclusters (AgNCs) heavily quenched the ECL signal for miRNA-21 detection. However, toxic components restrict the application of QDs in biological fields. Beneficial to the good biocompatibility and excellent stability, silver nanoclusters (AgNCs) and copper nanoclusters (CuNCs) have been commonly utilized in ECL biosensors. Moreover, nucleotides in DNA structure show high affinity towards metal ions to act as the template for the in-situ formation of NCs, for instance, thymine for copper ions and cytosine for silver ions. Liao et al. reported an ECL biosensor for the detection of miRNA-21 based on the in-situ electrochemically formed CuNCs as luminophore and AT-rich dsDNA as the template [37]. Sun et al. reported a multi-targeted ECL biosensor for myocardial miRNA detection by coupling of DNAzyme with cascading amplification [38]. As shown in Figure 6, sulfhydryl-functionalized versatile probe containing RNA splice sites was assembled on the AuNP-coated GCE. The myocardial miRNA targets were hybridized with the auxiliary strands to form circular structures which could form DNAzymes on the probe and cleavage the probe at the rA site. The products on the electrode initiated HCR and a long dsDNA chain was formed with a lot of C-rich sequences that acted as the templates for the in-situ generation of ECL AgNCs. The redox-active AgNCs can act as the labels in electrochemical analysis. For this consideration, Jie et al. reported a PEC and electrochemical aptasensor for thrombin detection by the in-situ synthesis of AgNCs as multifunctional labels [39]. In this work, under DNAzyme-assisted target recycling and HCR multiple amplification strategy, few thrombin could induce the formation of a large number of long dsDNA concatamers on the electrode surface. Then, numerous AgNCs were in-situ synthesized using the dsDNA with cytosine-rich loops as the templates, which could dramatically amplify the ECL and electrochemical signal. To further enhance the emission intensity of luminophores, plasmon-enhanced ECL has proved to be an effective pathway [40]. Liu et al. reported a distance-dependent plasmon-enhanced ECL biosensor by using nonmetallic MoS₂ nanosheets [41]. In this study, when the luminophore (sulfur doped boron nitrogen QDs) was close to the nanosheets, the ECL signal was quenched due to the ECL-resonant energy transfer. However, when the distance was increased, the ECL intensity from QDs was improved due to the plasmon-enhanced ECL.

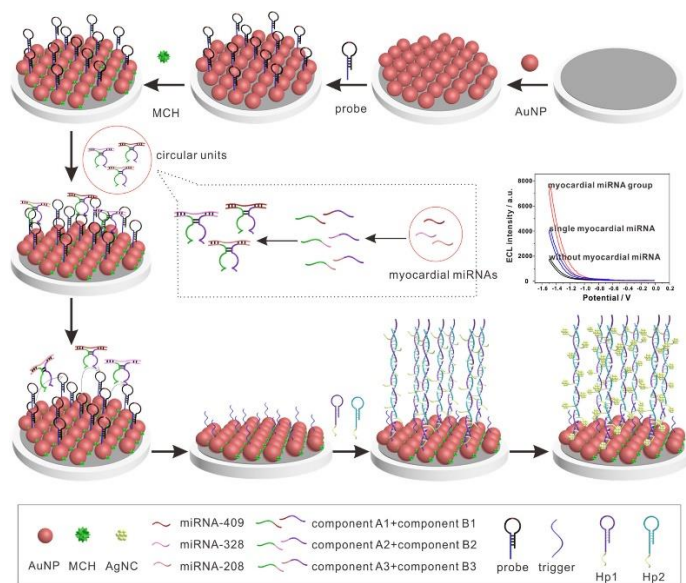


Figure 6. Schematic representation of the multitargeted ECL biosensor for analyzing myocardial miRNAs [38]. Copyright 2021 American Chemical Society.

Nanomaterials with high surface area can be employed as nanocarriers to load numerous redox labels and recognition elements. Therefore, a single hybridization event can be converted into hundreds of luminophores for improving the sensitivity and selectivity. For example, Wu et al. used gold nanoparticles (AuNPs) to load multiple luminol molecules and HCR primer DNA molecules [42]. Wu et al. developed an HCR-based ECL aptasensor for thrombin detection using europium multi-walled CNTs (Eu-MWCNTs) as the luminophores [43]. As displayed in Figure 7, MWCNTs with a hollow structure was used to load europium(III) complex through the coordination between europium(III) and bipyridine ligands. Two hairpins DNA strands were labeled with amino groups. Under the exonuclease-aided target recycling and HCR, the extended dsDNA would be formed on the electrode surface. Many Eu-MWCNTs as the luminophores were tethered onto the polymers through the amidation reaction between the amino of DNA and the carboxyl of Eu-MWCNTs, leading to an enhanced ECL signal.

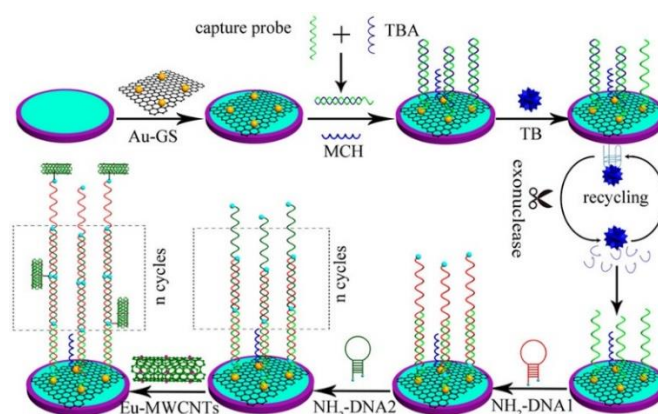


Figure 7. Schematic diagram of the proposed ECL-based aptasensor for TB detection [43]. Copyright 2015 American Chemical Society.

Nanomaterials can also be used to immobilize plenty of trigger probes and recognition elements (DNA, aptamers and antibodies). After the recognition reaction, triggers on NPs surface can initiate multiple HCR for signal amplification [44-48]. For instance, Bai et al. reported a label-free ECL biosensor for the detection of thymine DNA glycosylase activity using DNA-functionalized AuNPs-triggered HCR [49]. Nie et al. constructed a non-enzymatic ECL biosensor for multiple types of biomarkers detection [50]. As illustrated in Figure 8, DNA probe H1 was first immobilized on the $\text{TiO}_2@\text{Pt}$ modified electrode via a Pt-S covalent bond. Under the catalyst of catalytic hairpin assembly (CHA) reaction, target 1 miRNA-21 induced the immobilization of abundant H2-PtNPs-S1 bioconjugates on the electrode surface. Subsequently, doxorubicin (Dox) was added to intercalate into dsDNA for avoiding false positive signal. MUC1 protein aptamer was introduced to activate HCR amplification and numerous dsDNA polymers were in-situ generated on the nanoparticles to capture ECL emitters and produce enhanced ECL signal. When target 2 (MUC1 protein) was present, the complex of MUC1 and its aptamer resulted in the release of dsDNA polymers and led to a decreased ECL intensity, which realized the detection of MUC1 protein. Zhu et al. developed an ECL immunosensor for the detection of cardiac troponin I based on AuNCs and HCR signal amplification [51]. As presented in Figure 9, AuNPs were utilized as the nanocarriers of DNA initiator strands (T_1) and secondary antibody (Ab_2) ($Ab_2\text{-AuNP-}T_1$). AuNCs were employed as the luminophores to modify hairpin DNA (H_1 and H_2) at each ends. After the introduction of target, the formation of sandwich-like immunocomplex and HCR, a lot of AuNCs were immobilized on the sensing surface to generate a strong ECL signal in the presence of the coreactant ($\text{K}_2\text{S}_2\text{O}_8$).

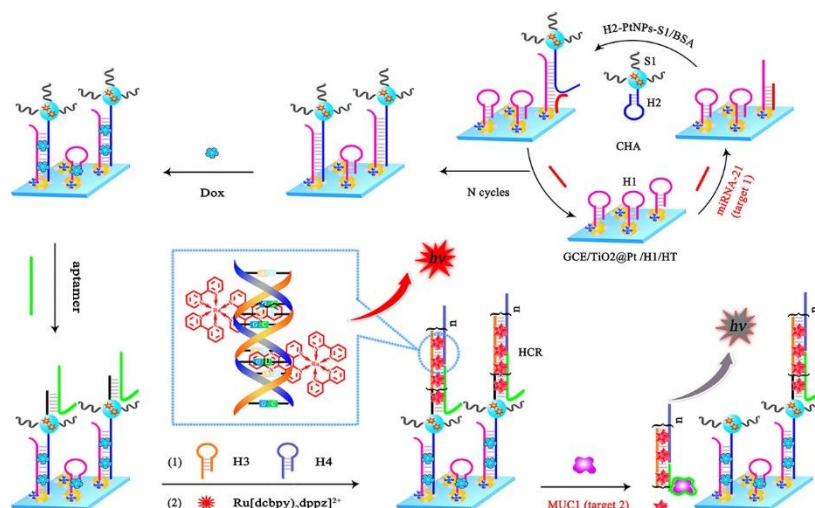


Figure 8. Schematic diagram of the versatile and ultrasensitive ECL biosensor for the monitoring of miRNA-21 and MUC1 from breast cancer [50]. Copyright 2019 American Chemical Society.

Recently, many researches have focused on the exploration of enzyme-mimetic nanomaterials (nanozymes) as labels for signal amplification in bioassays. Metallic alloy nanomaterials show higher enzyme-like activities than monometallic counterparts. Ge et al. presented a nanozyme and HCR-based ECL biosensor for the detection of tumor cells and evaluation of H_2O_2 [52]. In this study, AuPd NPs on the electrode surface not only served as the carriers of the capture aptamer, but also acted as the nanocatalyst for the ECL reaction of luminol and H_2O_2 .

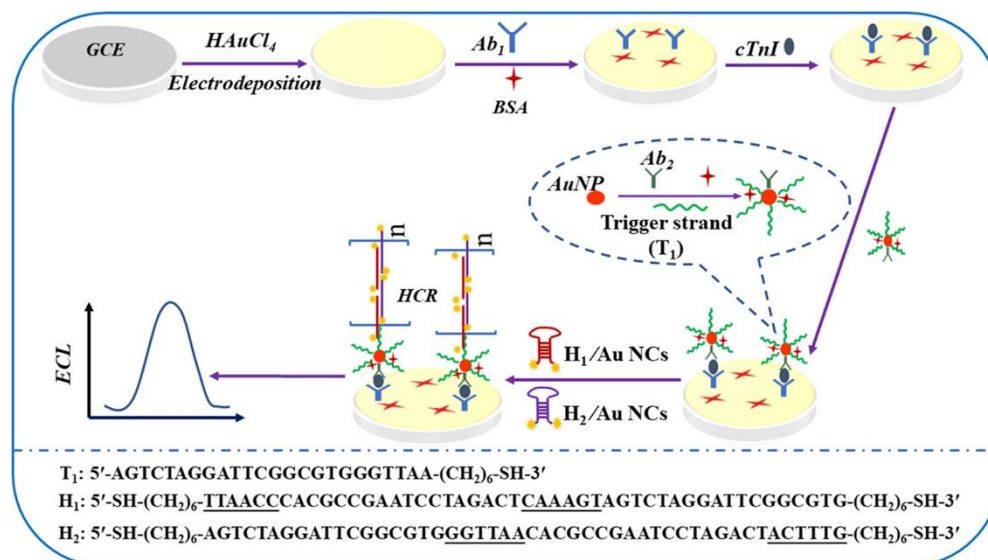


Figure 9. Schematic diagram of the ECL immunosensor for detection of cardiac troponin I based on AuNCs and HCR [51]. Copyright 2019 American Chemical Society.

3. CONCLUSION

HCR technology has the advantages of high sensitivity, good selectivity and simple operation, but it also faces many challenges. For example, although some researchers have considered the energy storage in hairpin design and the interaction between hairpin and target from the perspective of thermodynamics, there is still a lack of systematic reference guide for the structural design of hairpin. In addition, it is easy to produce high background signal, and it is difficult to achieve absolute quantization with HCR technique. Therefore, there is still a lot of work to be done in the application of HCR-based biosensors. It is desired to develop software which can directly design HCR hairpins with high amplification efficiency. The combination of HCR and enzyme-free nucleic acid signal amplification technology can be explored to realize multiple signal amplification, and some novel nanomaterials should be introduced to combine with HCR to improve the sensitivity.

ACKNOWLEDGMENTS

We acknowledge the financial support of the Science and Technology Foundation of Guizhou Province (Nos. 2021GZJ003 and QKHJC-ZK[2022]332), the Integrated Research Platform from Education Department of Guizhou Province (QJHKY(2020)008), and the Natural Science Foundation of Department of Education of Guizhou Province ([2021]021).

References

1. Y. Nie, X. Yuan, P. Zhang, Y. Chai and Y. R., *Anal. Chem.*, 91 (2019) 3452.
2. L. Hou and B. Zhou, *Int. J. Electrochem. Sci.*, 14 (2019) 2489.
3. Y. Feng and M. La, *Int. J. Electrochem. Sci.*, 17 (2022) 220252.

4. E. M. McConnell, I. Cozma, Q. Mou, J. D. Brennan, Y. Lu and Y. Li, *Chem. Soc. Rev.*, 50 (2021) 8954.
5. M. Li, F. Yin, L. Song, X. Mao, F. Li, C. Fan, X. Zuo and Q. Xia, *Chem. Rev.*, 121 (2021) 10469.
6. R. M. Dirks and N. A. Pierce, *Proc. Natl. Acad. Sci. USA*, 101 (2004) 15275.
7. Q. Zhang, *Int. J. Electrochem. Sci.*, 17 (2022) 220227.
8. H. Chai, W. Cheng, D. Jin and P. Miao, *ACS Appl. Mater. Interfaces*, 13 (2021) 38931.
9. C. Zhang, J. Chen, R. Sun, Z. Huang, Z. Luo, C. Zhou, M. Wu, Y. Duan and Y. Li, *ACS Sens.*, 5 (2020) 2977.
10. D. Liu, G. Yang, X. Zhang, S. Chen and R. Yuan, *Sens. Actua. B: Chem.*, 329 (2021) 129210.
11. J. Zhao, J. Luo, D. Liu, Y. He, Q. Li, S. Chen and R. Yuan, *Sens. Actua. B: Chem.*, 316 (2020) 128139.
12. L. Xiao, Y. Chai, R. Yuan, Y. Cao, H. Wang and L. Bai, *Talanta*, 115 (2013) 577.
13. M. Zhao, Y. Zhuo, Y. Chai, Y. Xiang, N. Liao, G. Gui and R. Yuan, *Analyst*, 138 (2013) 6639.
14. G. Liu, Y. Yuan and J. Wang, *RSC Adv.*, 6 (2016) 37221.
15. B. Jiang, M. Yang, C. Yang, Y. Xiang and R. Yuan, *Sens. Actua. B: Chem.*, 247 (2017) 573.
16. R. Zhang, A. Chen, Y. Yu, Y. Chai, Y. Zhuo and R. Yuan, *Microchim. Acta*, 185 (2018) 432.
17. W. J. Zeng, N. Liao, Y. M. Lei, J. Zhao, Y. Q. Chai, R. Yuan and Y. Zhuo, *Biosens. Bioelectron.*, 100 (2018) 490.
18. L. Zhu, L. Yu, J. Ye, M. Yan, Y. Peng, J. Huang and X. Yang, *Biosens. Bioelectron.*, 178 (2021) 113022.
19. W. Liang, C. Fan, Y. Zhuo, Y. Zheng, C. Xiong, Y. Chai and R. Yuan, *Anal. Chem.*, 88 (2016) 4940-4948.
20. L. Zhu, J. Ye, S. Wang, M. Yan, Q. Zhu, J. Huang and X. Yang, *Chem. Commun.*, 55 (2019) 11551.
21. X. Zhang, W. Li, Y. Zhou, Y. Chai and R. Yuan, *Biosens. Bioelectron.*, 135 (2019) 8.
22. X. Wang, S. Xiao, C. Yang, C. Hu, X. Wang, S. Zhen, C. Huang and Y. Li, *Anal. Chem.*, 93 (2021) 14178.
23. Y. Li, C. Z. Huang and Y. F. Li, *Anal. Chem.*, 91 (2019) 9308.
24. Y. Xiong, L. Lin, X. Zhang and G. Wang, *RSC Adv.*, 6 (2016) 37681.
25. Y. Lin, J. Wang, F. Luo, L. Guo, B. Qiu and Z. Lin, *Electrochim. Acta*, 283 (2018) 798.
26. Q. Zhang, T. Hao, D. Hu, Z. Guo, S. Wang and Y. Hu, *Electrochim. Acta*, 356 (2020) 136828.
27. Y. Xu, Y. Xu, Z. Zuo, X. Zhou, B. Guo, Y. Sang and S. Ding, *J. Electroanal. Chem.*, 801 (2017) 192.
28. H. Zhang, F. Luo, P. Wang, L. Guo, B. Qiu and Z. Lin, *Biosens. Bioelectron.*, 129 (2019) 36.
29. L. Lu, J. Wang, W. Miao, X. Wang and G. Guo, *Anal. Chem.*, 91 (2019) 1452.
30. X. Huang, Y. Zhang, W. Xu, W. Xu, L. Guo, B. Qiu and Z. Lin, *Chem. Commun.*, 55 (2019) 12980.
31. Y. Xu, Y. Zhang, X. Sui, A. Zhang, X. Liu, Z. Lin and J. Chen, *Sens. Actua. B: Chem.*, 344 (2021) 130226.
32. X. Huang, J. Jia, Y. Lin, B. Qiu, Z. Lin and H. Chen, *ACS Appl. Mater. Interfaces*, 12 (2020) 34716.
33. X. Huang, X. Bian, L. Chen, L. Guo, B. Qiu and Z. Lin, *Anal. Chem.*, 93 (2021) 10351.
34. J. Wang, L. Zhang, L. Lu and T. Kang, *Microchim. Acta*, 186 (2019) 142.
35. G. Jie and G. Jie, *RSC Adv.*, 6 (2016) 24780.
36. J. Ge, C. Li, Y. Zhao, X. Yu and G. Jie, *Chem. Commun.*, 55 (2019) 7350.
37. H. Liao, Y. Zhou, Y. Chai and R. Yuan, *Biosens. Bioelectron.*, 114 (2018) 10.
38. Y. Sun, Fang, Z. Zhang, Y. Yi, S. Liu, Q. Chen, J. Zhang, C. Zhang, L. He and K. Zhang, *Anal. Chem.*, 93 (2021) 7516.
39. G. Jie, L. Tan, Y. Zhao and X. Wang, *Biosens. Bioelectron.*, 94 (2017) 243.
40. H. Zhang, Z. Guo, H. Dong, H. Chen and C. Cai, *Analyst*, 142 (2017) 2013.

41. Y. Liu, Y. Nie, M. Wang, Q. Zhang and Q. Ma, *Biosens. Bioelectron.*, 148 (2020) 111823.
42. H. Wu, Y. Su, J. Jiang, Y. Liang and C. Zhang, *J. Lumin.*, 226 (2020) 117485.
43. D. Wu, X. Xin, X. Pang, M. Pietraszkiewicz, R. Hozyst, X. Sun and Q. Wei, *ACS Appl. Mater. Interfaces*, 7 (2015) 12663.
44. J. Lu, L. Wu, Y. Hu, S. Wang and Z. Guo, *Biosens. Bioelectron.*, 109 (2018) 13.
45. H. Hai, C. Chen, D. Chen, P. Li, Y. Shan and J. Li, *Microchim. Acta*, 188 (2021) 125.
46. Y. Sun, Y. Qin, J. Zhang and Q. Ren, *Microchim. Acta*, 188 (2021) 300.
47. G. Gui, Y. Zhuo, Y. Q. Chai, N. Liao, M. Zhao, J. Han, Q. Zhu, R. Yuan and Y. Xiang, *Biosens. Bioelectron.*, 47 (2013) 524.
48. W. Yang, Q. Peng, Z. Guo, H. Wu, S. Ding, Y. Chen and M. Zhao, *Biosens. Bioelectron.*, 142 (2019) 111548.
49. W. Bai, Y. Wei, Y. Zhang, L. Bao and Y. Li, *Anal. Chim. Acta*, 1061 (2019) 101.
50. Y. Nie, X. Yuan, P. Zhang, Y. Q. Chai and R. Yuan, *Anal. Chem.*, 91 (2019) 3452.
51. L. Zhu, J. Ye, M. Yan, Q. Zhu, S. Wang, J. Huang and X. Yang, *ACS Sens.*, 4 (2019) 2778.
52. S. Ge, J. Zhao, S. Wang, F. Lan, M. Yan and J. Yu, *Biosens. Bioelectron.*, 102 (2018) 411.

© 2022 The Authors. Published by ESG (www.electrochemsci.org). This article is an open access article distributed under the terms and conditions of the Creative Commons Attribution license (<http://creativecommons.org/licenses/by/4.0/>).